# Wavelength convergence of the E × B staircase pattern in flux tube simulations of ion temperature gradient driven turbulence

M. Lippert,[1, a)] F. Rath,[1, b)] and A. G. Peeters[1]

*Physics Department, University of Bayreuth, 95440 Bayreuth, Germany*

(*Electronic mail: Florian.Rath@uni-bayreuth.de)

(Dated: 21 March 2023)

The wavelength convergence of the E × B staircase pattern is adressed in local gradient-driven flux tube simulations of ion temperature gradient (ITG) driven turbulence. Its is shown that a mesoscale pattern wavelength of $\sim 57.20 - 76.27\,\rho$ is inherent to ITG driven turbulence with Cyclone Base Case parameters in the local limit.

Ion temperature gradient driven turbulence close to marginal stability often exhibits zonal flow pattern formation on mesoscales, so-called E × B staircase structures[1]. Such pattern formation has been observed in local gradient-driven flux-tube simulations[2–4] as well as global gradient-driven[5–7] and global flux-driven[1,8–11] studies. In global studies, usually spanning a larger fraction of the minor radius, multiple radial repetitions of staircase structures are usually observed, with a typical pattern wavelength of several ten Larmor radii. By contrast, in the aforementioned local studies the wavelength of E × B staircase structures is always found to converge to the radial box size of the flux tube domain. The above observations lead to the question: *Does the basic pattern wavelength always converges to the box size, or is there a typical mesoscale wavelength inherent to staircase structures also in a local flux-tube description?* The latter case would imply that it is not necessarily global physics which means profile effects are usually restricted to E × B staircase structures and considered as a nonlocal transport mechanism. This profile effects set (i) the wavelength of the E × B staircase pattern and (ii) the scale of avalanche-like transport events[1]. In this brief communication the above question is addressed through a box size convergence scan of the same cases close to the nonlinear threshold for turbulence generation as studied in Ref.[2].

Here, gyrokinetic simulations are performed with the nonlinear flux tube version of Gyrokinetic Workshop (GKW)[12] in the adiabatic electron approximation. In agreement with Ref.[2], Cyclone Base Case (CBC) like parameters are chosen with an inverse background temperature gradient length $R/L_T = 6.0$ and circular concentric flux surfaces. The numerical resolution is compliant to the "Standard resolution with 6th order (S6)" set-up of the aforementioned reference, with a somewhat lowered number of parallel velocity grid points. It has been carefully verified that this modification preserves the same physical outcome as the original study. A summary of the numerical parameters is given in Tab. I and for more details about the definition of individual quantities the reader is referred to Refs.[2,12].

| | $N_m$ | $N_x$ | $N_s$ | $N_{v_\parallel}$ | $N_\mu$ | $D$ | $v_d$ | $D_{v_\parallel}$ | $D_x$ | $D_y$ | Order | $k_y\rho$ | $k_x\rho$ |
|---|---|---|---|---|---|---|---|---|---|---|---|---|---|
| S6 | 21 | 83 | 16 | 48 | 9 | 1 | $|v_\parallel|$ | 0.2 | 0.1 | 0.1 | 6 | 1.4 | 2.1 |

TABLE I: Resolution used in this paper for further information the author links to Ref.[2].

The increase of the box size, relative to the standard box size $(L_x, L_y) = (76.27, 89.76)\,\rho$, in the radial and binormal direction is always indicated by the real parameter $N_R$ and $N_B$, respectively. Here, the nomenclature $N_R \times N_B$ is applied throughout this work to indicate the increase in box size. Note that the number of modes in the respective direction is always adapted accordingly to retain a spatial resolution compliant to the standard resolution [Tab. I] and standard box size.

The E × B staircase pattern is manifest as radial structure formation in the E × B shearing rate defined by[2,13,14]

$$\omega_{E\times B} = \frac{1}{2}\frac{\partial^2\langle\phi\rangle}{\partial x^2}, \tag{1}$$

where $\langle\phi\rangle$ is the zonal electrostatic potential normalized by $\rho_* T/e$ ($\rho_* = \rho/R$ is the thermal Larmor radius normalized with the major radius $R$, $T$ is the temperature, $e$ is the elementary charge) and $x$ is the radial coordinate that labels the flux surfaces normalized by $\rho$. Consistent with Ref.[2] the turbulence level is quantified by the turbulent heat conduction coefficient $\chi$, which is normalized by $\rho^2 v_{th}/R$ ($v_{th} = \sqrt{2T/m}$ is the thermal velocity and $m$ is the mass). Furthermore, quantities $\rho$, $R$, $T$, $v_{th}$ and $m$ are referenced quantities from Ref(?). The zonal potential is estimated from the electrostatic potential $\phi$ on the two-dimensional $x$-$y$-plane at the low field side according to

$$\langle\phi\rangle = \frac{1}{L_y}\int_0^{L_y} \mathrm{d}y\,\phi(x,y,s=0), \tag{2}$$

where $y$ labels the field lines and is an approximate binormal or toroidal coordinate, and $s$ parameterizes the length along the field lines and represents a poloidal coordinate which represents together with the radial coordinate $x$ the Hamada coordinates $(x,y,s)$.[4](?) The E×B shearing rate $\omega_{E\times B}$ is the radial derivative of the advecting zonal flow velocity[15,16] and quantifies the zonal flow induced shearing of turbulent structures[15,17,18].

In order to diagnose the temporal evolution of the staircase pattern and to obtain an estimate of its amplitude the radial Fourier transform of the E × B shearing rate is considered. It is defined by

$$\omega_{E\times B} = \sum_{k_{ZF}} \widehat{\omega}_{E\times B}(k_{ZF}, t)\exp(ik_{ZF}x), \qquad (3)$$

where $\widehat{\omega}_{E\times B}$ is the complex Fourier coefficient and $k_{ZF} = 2\pi n_{ZF}/L_x$ defines the zonal flow wave vector with the zonal flow mode number $n_{ZF}$ ranging in $-(N_x-1)/2 \leq n_{ZF} \leq (N_x-1)/2$. Based on the definitions above, the shear carried by the zonal flow mode with wave vector $k_{ZF}$ is defined by $|\widehat{\omega}_{E\times B}|_{k_{ZF}} = 2|\widehat{\omega}_{E\times B}|$. In general, the zonal flow mode that dominates the E × B staircase pattern, also referred to as the *basic mode* of the pattern in this work, exhibits the maximum amplitude in the spectrum $|\widehat{\omega}_{E\times B}|_{k_{ZF}}$.

In the first test the radial box size is increased while the binormal box size is kept fixed to the standard size. The scan covers the realizations $N_R \times N_B \in [1 \times 1, 2 \times 1, 3 \times 1, 4 \times 1]$. Each realization exhibits an initial quasi-stationary turbulent phase and a second final[2] phase with almost suppressed turbulence [Fig. 1 (a)]. The latter state is indicative for the presence of a fully developed staircase pattern as depicted in Fig. 2. This type of structure is characterized by intervals of almost constant shear with alternating sign satisfying the Waltz criterion $|\omega_{E\times B}| \approx \gamma^{16,19}$ ($\gamma$ is the growth rate of the most unstable linear ITG driven Eigenmode), connected by steep flanks where $\omega_{E\times B}$ crosses zero. Fig. 2 (a) shows a striking repetition of the staircase structure, with the number of repetitions equal to $N_R$. Hence, the basic wavelength of the pattern not only converges with increasing radial box size, the converged wavelength turns out to agree with the standard radial box size of Ref.[2]

Due to the lack of a substantial turbulent drive in the final suppressed state no further zonal flow evolution is observed [Fig. 1 (b)] and one might critically ask whether the structures shown in Fig. 2 represent the real converged pattern in a statistical sense. Note that in the 3 × 1 case the initial quasi-stationary turbulent state extends up to a few $\sim 10^4 R/v_{th}$. During this period the zonal flow mode with $n_{ZF} = 3$, i.e., the mode that dominates the staircase pattern in final suppressed phase, undergoes a long-term evolution with a typical time scale of several $\sim 10^3 R/v_{th}$. Hence, several of such cycles are covered by the initial turbulent phase, which is evident from the occurrence of phases with reduced amplitude around $t \approx 8000 R/v_{th}$ and $t \approx 18000 R/v_{th}$. It is the $n_{ZF} = 4$ zonal flow mode, i.e., the next shorter radial scale mode, that dominates the shear spectrum $|\widehat{\omega}_{E\times B}|_k$ in the latter two phases (not shown), demonstrating a competition between the $n_{ZF} = 3$ and $n_{ZF} = 4$ modes. Most importantly, no secular growth of the $n_{ZF} = 1$ (box scale) zonal flow mode is observed during the entire quasi-stationary turbulent phase [Fig. 1 (b) dotted line]. The above discussion indicates that although the $n_{ZF} = 3, 4$ zonal modes compete, the pattern scale does not converge to the radial box scale but rather to a mesoscale of $\sim 57.20 - 76.27 \rho$ (i.e., $n_{ZF} = 4, 3$ in the 3 × 1 case).

Since the radially elongated simulation domain might inhibit the development of isotropic turbulent structures, in the second test the radial and binormal box size is increased simultaneously. This scan covers the realizations $N_R \times N_B \in [1 \times 1, 2 \times 2, 3 \times 3]$. Interestingly, here, suppression of the turbulence by the emergence of a fully developed staircase pattern occurs after $\sim 1000 R/v_{th}$ always [Fig. 3], i.e., significantly faster compared to the 3 × 1 and 4 × 1 realizations. As shown in Fig. 2 (b) also this test confirms the convergence of the staircase pattern wavelength to a typical mesoscale that is distinct from the radial box size in the $N_R > 1$ realizations.
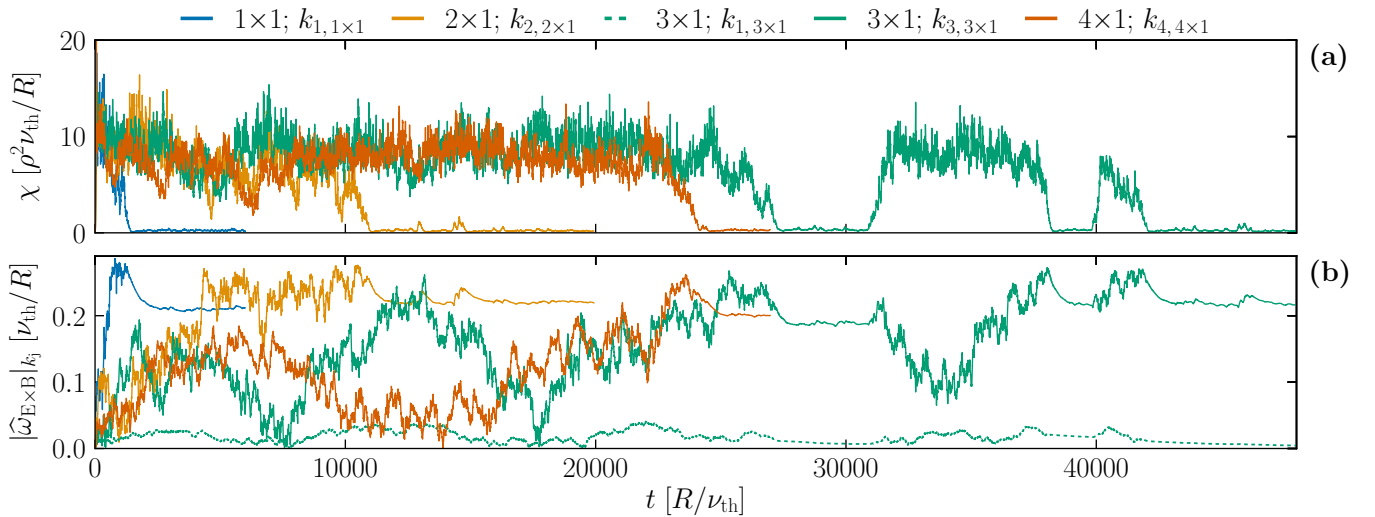


FIG. 1: **(a)** Time traces of the heat conduction coefficient $\chi$ for $R/L_T = 6.0$ for radial increased box sizes
**(b)** Time traces of $|\widehat{\omega}_{E\times B}|_{k_{ZF}}$ for radial increased box sizes
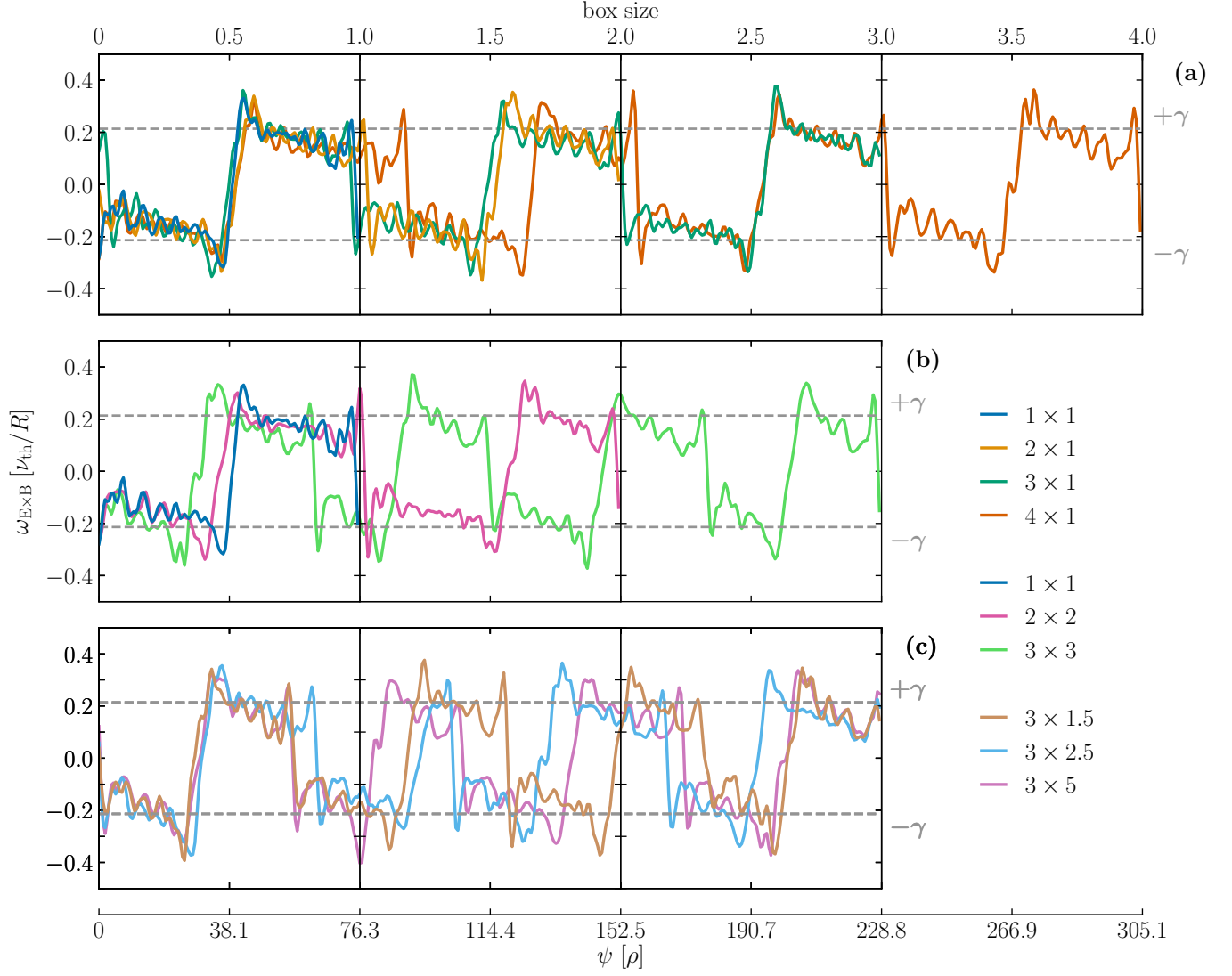
FIG. 2: Comparison of shearing rate $\omega_{E \times B}$ for each box sizes scan averaged over time interval and the growth rate $\pm\gamma$ of the most unstable linear ITG driven Eigenmode. The staircase structures got shifted till alignment for better visibility.
**(a) radial:**    $t_{1 \times 1} \in [2000, 5000]$, $t_{2 \times 1} \in [15000, 18000]$, $t_{3 \times 1} \in [43000, 45000]$, $t_{4 \times 1} \in [26000, 28000]$
**(b) isotropic:** $t_{1 \times 1} \in [2000, 5000]$, $t_{2 \times 2} \in [2000, 3000]$,    $t_{3 \times 3} \in [2000, 3000]$
**(c) binormal:** $t_{3 \times 1.5} \in [2000, 3000]$, $t_{3 \times 2.5} \in [2000, 3000]$,    $t_{3 \times 5} \in [1000, 3000]$
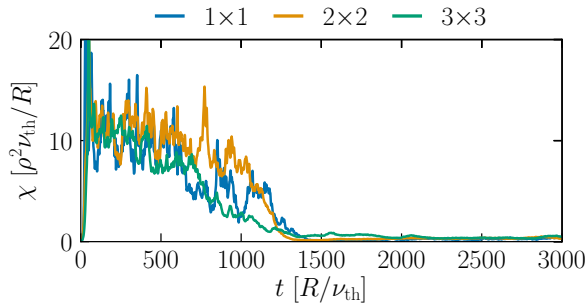


FIG. 3: Time traces of the heat conduction coefficient $\chi$ for $R/L_T = 6.0$ for isotropic increased box sizes

By contrast to the radial box size scan, however, here the $3 \times 3$ realization shows a stationary pattern with four repetitions of the fully developed staircase structure, i.e., a somewhat smaller pattern wavelength. Whether this is related to a possible pattern wavelength dependence on the binormal box size or to the competition between patterns with the two wavelengths $\lambda \in [57.20, 76.27]\,\rho$ as observed in the first test is addressed in the next paragraph.

In a third test the binormal box size is varied with the radial box size fixed to $N_R = 3$. This test covers the realizations $N_R \times N_B \in [3 \times 1.5, 3 \times 2.5, 3 \times 3, 3 \times 5]$. As in the isotropic scan the turbulence subdued and a fully developed staircase pattern formats always after $\sim 2000\,R/v_{\text{th}}$ [Fig. 4]. The convergence of staircase pattern can be seen in Fig. 2 (c) and the

test confirms again the typical mesoscale distinct from $N_R > 1$. Fig. 2 (c) also confirms that indeed a competition between patterns with two wavelengths $\lambda \in [57.20, 76.27]\rho$ causing the different results for $3 \times 1$ and $3 \times 3$. The zonal flow mode number varies between $n_{ZF} = [3, 4]$ which can be seen in Fig. 2 (c). For the realization $3 \times 2.5$ the staircase structure has an pattern between 3 and 4 repetitions which get represented in the second repetition with no $+\gamma$ interval. Instead the pattern returns immediately after reaching $+\gamma$ to the $-\gamma$ interval of the third repetition. The Fourier analysis yields in this case no definitely basic mode rather two dominate modes with $n_{ZF} = 3, 4$ with a fraction of the maximum amplitude $|\widehat{\omega}_{E \times B}|_{k_{ZF}}$ each.
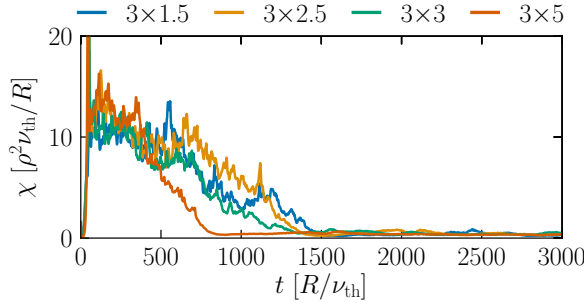


FIG. 4: Time traces of the heat conduction coefficient $\chi$ for $R/L_T = 6.0$ for binormal increased box sizes

In the final test the inverse background temperature gradient length $R/L_T$ is varied at fixed $3 \times 3$ box size. Since suppression of turbulence usually occurs at later times when approaching the finite heat flux threshold from below[2], the analysis aims to lengthen the phase during which the zonal flow varies in time due to turbulent Reynolds stresses. This scan covers realizations with $R/L_T \in [6.0, 6.2, 6.4]$. In the case of $R/L_T = 6.2$ turbulence suppression is observed for $t > 12000 R/v_{th}$, while stationary turbulence during the entire simulation time trace of $12000 R/v_{th}$ is found for $R/L_T = 6.4$. The finite heat flux threshold, hence, is $R/L_T|_{finite} = 6.4 \pm 0.1$. Although the initial quasi-stationary turbulence in the former case is significantly larger compared to the $R/L_T = 6.0$ realization discussed in the second test, a stationary pattern with basic zonal flow mode $n_{ZF} = 3$ establishes. Again, the $n_{ZF} = 1$ (box scale) zonal flow mode does not grow secularly during the entire turbulent phase. Also, this test confirms the statistical soundness of the converged pattern wavelength of $\sim 57.20 - 76.27\rho$.

Through careful tests this brief communication confirms the wavelength convergence of the E × B staircase pattern in local gyrokinetic flux tube simulations of ion temperature gradient (ITG) driven turbulence. A mesoscale pattern wavelength of $\sim 57.20 - 76.27\rho$ is found to be intrinsic to ITG driven turbulence for Cyclone Base Case parameters. This length scale is somewhat larger compared to results from global studies with finite $\rho_*$, which report of a few $10\rho$[1], and has to be considered the proper mesoscale in the local limit $\rho_* \to 0$. The occurrence of this mesoscale implies that non-locality is inherent to ITG driven turbulence, since avalanches are usually spatially organized by the E × B staircase pattern[1,2,5,13].

[1]G. Dif-Pradalier, P. H. Diamond, V. Grandgirard, Y. Sarazin, J. Abiteboul, X. Garbet, P. Ghendrih, A. Strugarek, S. Ku, and C. S. Chang, Phys. Rev. E **82**, 025401 (2010).

[2]A. G. Peeters, F. Rath, R. Buchholz, Y. Camenen, J. Candy, F. J. Casson, S. R. Grosshauser, W. A. Hornsby, D. Strintzi, and A. Weikl, "Gradient-driven flux-tube simulations of ion temperature gradient turbulence close to the non-linear threshold," Phys. Plasmas **23**, 082517 (2016).

[3]A. Weikl, A. G. Peeters, F. Rath, S. R. Grosshauser, R. Buchholz, W. A. Hornsby, F. Seiferling, and D. Strintzi, "Ion temperature gradient turbulence close to the finite heat flux threshold," Phys. Plasmas **24**, 102317 (2017).

[4]F. Rath, A. G. Peeters, and A. Weikl, "Analysis of zonal flow pattern formation and the modification of staircase states by electron dynamics in gyrokinetic near marginal turbulence," Phys. Plasmas **28**, 072305 (2021).

[5]B. F. McMillan, S. Jolliet, T. M. Tran, L. Villard, A. Bottino, and P. Angelino, "Avalanchelike bursts in global gyrokinetic simulations," Physics of Plasmas **16**, 022310 (2009), https://doi.org/10.1063/1.3079076.

[6]L. Villard, P. Angelino, A. Bottino, S. Brunner, S. Jolliet, B. F. McMillan, T. M. Tran, and T. Vernay, "Global gyrokinetic ion temperature gradient turbulence simulations of iter," Plasma Physics and Controlled Fusion **55**, 074017 (2013).

[7]J. Seo, H. Jhang, and J.-M. Kwon, "Effects of light impurities on zonal flow activities and turbulent thermal transport," Physics of Plasmas **29**, 052502 (2022), https://doi.org/10.1063/5.0086587.

[8]G. Dif-Pradalier, G. Hornung, P. Ghendrih, Y. Sarazin, F. Clairet, L. Vermare, P. H. Diamond, J. Abiteboul, T. Cartier-Michaud, C. Ehrlacher, D. Estève, X. Garbet, V. Grandgirard, O. D. Gürcan, P. Hennequin, Y. Kosuga, G. Latu, P. Maget, P. Morel, C. Norscini, R. Sabot, and A. Storelli, "Finding the elusive E × B staircase in magnetized plasmas," Phys. Rev. Lett. **114**, 085004 (2015).

[9]W. Wang, Y. Kishimoto, K. Imadera, H. Liu, J. Li, M. Yagi, and Z. Wang, "Statistical study for itg turbulent transport in flux-driven tokamak plasmas based on global gyro-kinetic simulation," Nuclear Fusion **60**, 066010 (2020).

[10]Y. J. Kim, K. Imadera, Y. Kishimoto, and T. S. Hahm, "Transport events and e×b staircase in flux-driven gyrokinetic simulation of ion temperature gradient turbulence," Journal of the Korean Physical Society **81**, 636 (2022).

[11]Y. Kishimoto, K. Imadera, A. Ishizawa, W. Wang, and J. Q. Li, "Characteristics of constrained turbulent transport in flux-driven toroidal plasmas," Philosophical Transactions of the Royal Society A: Mathematical, Physical and Engineering Sciences **381**, 20210231 (2023), https://royalsocietypublishing.org/doi/pdf/10.1098/rsta.2021.0231.

[12]A. G. Peeters, Y. Camenen, F. J. Casson, W. A. Hornsby, A. P. Snodin, D. Strintzi, and G. Szepesi, Comput. Phys. Commun. **180**, 2650 (2009).

[13]F. Rath, A. G. Peeters, R. Buchholz, S. R. Grosshauser, P. Migliano, A. Weikl, and D. Strintzi, "Comparison of gradient and flux driven gyrokinetic turbulent transport," Phys. Plasmas **23**, 052309 (2016).

[14]M. J. Pueschel, M. Kammerer, and F. Jenko, Physics of Plasmas **15**, 102310 (2008).

[15]T. S. Hahm and K. H. Burrell, "Flow shear induced fluctuation suppression in finite aspect ratio shaped tokamak plasma," Phys. Plasmas **2**, 1648–1651 (1995).

[16]R. E. Waltz, R. L. Dewar, and X. Garbet, Phys. Plasmas **5**, 1784–1792 (1998).

[17]H. Biglari, P. H. Diamond, and P. W. Terry, Phys. Fluids B: Plasma Physics **2**, 1–4 (1990).

[18]K. H. Burrell, Phys. Plasmas **4**, 1499–1518 (1997).

[19]R. E. Waltz, G. D. Kerbel, and J. Milovich, Phys. Plasmas **1**, 2229 (1994).